

**SYNTHESIS AND MESOMORPHIC PROPERTIES  
OF BENT-SHAPED 1,4-DISUBSTITUTED  
TRIAZOLE-CORED SCHIFF BASE WITH  
LATERAL ETHOXY GROUP**

**SITI NORHAZWANI BINTI ISMAIL**

**UNIVERSITI SAINS MALAYSIA**

**2024**

**SYNTHESIS AND MESOMORPHIC PROPERTIES  
OF BENT-SHAPED 1,4-DISUBSTITUTED  
TRIAZOLE-CORED SCHIFF BASE WITH  
LATERAL ETHOXY GROUP**

by

**SITI NORHAZWANI BINTI ISMAIL**

**Thesis submitted in fulfilment of the requirements  
for the degree of  
Master of Science**

**September 2024**

## ACKNOWLEDGEMENT

I extend my sincere appreciation to several individuals who have been pivotal in the completion of this thesis. My heartfelt gratitude goes to my main supervisor, Prof. Dr. Yeap Guan Yeow, whose guidance, support, and expertise have been invaluable throughout the entire research journey. I am also grateful to my current main supervisor, Associate Prof. Dr. Mohd Rizal Razali for his assistance, guidance, and support throughout the time after the retirement of my main supervisor. I am thankful for the resources and conducive environment provided by School of Chemical Sciences. Special thanks to my family for their unwavering encouragement and understanding. I also acknowledge my lab mates, Nur Fatin Liyana, Nur Amanina Juniasari, Yap Pui Wing and Nur Syaza Atikah for their insightful discussions, feedback, and help. Additionally, I am grateful to Prof. Masato Ito and team from Soka University, Japan for their collaborative support and aid. Their contribution has played a crucial role in the successful completion of this project. Besides, to the joint-collaborator from Yemen, Dr. Arwa Alshargaby, I would like to express gratitude for your guidance in my laboratory and experimental works. To all those who have made a meaningful impact on my academic and personal development during this time, my close friends, Najwa Najihah, Nurul Hidayah Idris and Nadiatul Asma, I express my deepest appreciation. Your support has been instrumental, and I am truly thankful for the role each of you has played in bringing this thesis to fruition.

## TABLE OF CONTENTS

<b>ACKNOWLEDGEMENT .....</b>	<b>ii</b>
<b>TABLE OF CONTENTS.....</b>	<b>iii</b>
<b>LIST OF TABLES .....</b>	<b>viii</b>
<b>LIST OF FIGURES .....</b>	<b>x</b>
<b>LIST OF SYMBOLS .....</b>	<b>xv</b>
<b>LIST OF ABBREVIATIONS .....</b>	<b>xvii</b>
<b>ABSTRAK .....</b>	<b>xx</b>
<b>ABSTRACT .....</b>	<b>xxii</b>
<b>CHAPTER 1 INTRODUCTION.....</b>	<b>1</b>
1.1 Overview .....	1
1.2 Bent-shaped/Banana-shaped Liquid Crystals (BLCs).....	1
1.3 Liquid Crystalline Compounds with [1,2,3]-Triazole Core .....	4
1.4 Problem Statement .....	5
1.5 Objectives.....	7
1.6 Research Scope .....	8
<b>CHAPTER 2 LITERATURE REVIEW.....</b>	<b>10</b>
2.1 State of Matter .....	10
2.2 Introduction to Liquid Crystals .....	11
2.3 Molecular Building Blocks/Liquid Crystal Constituents .....	15
2.3.1 Mesogenic Core.....	16
2.3.2 Flexible Chain .....	17
2.3.3 Linking Group .....	18
2.3.4 Terminal Group .....	19
2.3.5 Lateral Group .....	20
2.3.6 Triazole Core in Liquid Crystals .....	21

2.4	Types of Liquid Crystals .....	24
2.4.1	Lyotropic Liquid Crystals .....	24
2.4.2	Thermotropic Liquid Crystals .....	25
2.5	Conventional Liquid Crystals.....	26
2.5.1	Calamitic/Rod-like Liquid Crystals .....	27
2.5.2	Discotic/Disc-Shaped Liquid Crystals .....	28
2.6	Non-conventional Liquid Crystals .....	28
2.6.1	Oligomeric Liquid Crystals.....	29
2.6.2	Dimeric Liquid Crystals .....	29
2.6.3	Banana-shaped Liquid Crystals.....	30
2.7	Types of Liquid Crystal Phases.....	34
2.7.1	Nematic Phase .....	34
2.7.2	Smectic Phase.....	35
2.7.3	Columnar Phase.....	37
2.7.4	Banana Phase/B Phase .....	38
2.7.5	Polar Smectic and Frustrated Mesophase .....	39
2.8	Density Functional Theory .....	41
<b>CHAPTER 3 METHODOLOGY.....</b>		<b>43</b>
3.1	Chemicals .....	43
3.2	Characterization .....	43
3.3	Synthesis.....	45
3.3.1	Synthesis of Bent-Monomeric Triazole-cored Liquid Crystals, 4aA – 4dA and 4aB – 4dB .....	45
3.3.1(a)	Synthesis of 3-ethoxy-4-(prop-2-yn-1-yloxy) benzaldehyde, 1 .....	47
3.3.1(b)	Synthesis of ( <i>E</i> )-4'-((3-ethoxy-4-(prop-2-yn-1- yloxy)benzylidene)-[1,1'-biphenyl]-4-carbonitrile, 2A .....	47

3.3.1(c)	Synthesis of ( <i>E</i> )-4'-(3-ethoxy-4-(prop-2-yn-1-yloxy)benzylidene)-4-methoxyphenyl, 2B .....	47
3.3.1(d)	Synthesis of 1-azidononane, 3a .....	47
3.3.1(e)	Synthesis of 1-azidoundecane, 3b.....	48
3.3.1(f)	Synthesis of 1-azidododecane, 3c.....	48
3.3.1(g)	Synthesis of 1-azidohexadecane, 3d .....	48
3.3.1(h)	Synthesis of ( <i>E</i> )-4'-((3-ethoxy-4-((1-alkyl-1H-1,2,3-triazol-4-yl)methoxy)benzylidene)-[1,1'-biphenyl]-4-carbonitrile, 4aA – 4dA .....	48
3.3.1(i)	Synthesis of ( <i>E</i> )-4'-(3-ethoxy-4-((1-alkyl-1H-1,2,3-triazol-4-yl)methoxy)benzylidene)-4-methoxyphenyl, 4aB – 4dB .....	49
3.3.2	Synthesis of Bent-Dimeric Triazole-cored Liquid Crystals, 8aA – 8fA and 8aB – 8fB.....	50
3.3.2(a)	Synthesis of 3-ethoxy-4-(prop-2-yn-1-yloxy) benzaldehyde, 1 .....	52
3.3.2(b)	Synthesis of ( <i>E</i> )-4'-((3-ethoxy-4-(prop-2-yn-1-yloxy) benzylidene) amino)-[1,1'-biphenyl]-4-carbonitrile, 2A .....	52
3.3.2(c)	Synthesis of ( <i>E</i> )-4'-(3-ethoxy-4-(prop-2-yn-1-yloxy) benzylidene)-4-methoxyphenyl, 2B .....	52
3.3.2(d)	Synthesis of 2-methylbutyl-4'-hydroxy-[1,1'-biphenyl]-4-carboxylate, 5.....	52
3.3.2(e)	Synthesis of 2-methylbutyl-4'-(bromoheptyloxy)-[1,1'-biphenyl]-4-carboxylate, 6a .....	52
3.3.2(f)	Synthesis of 2-methylbutyl-4'-(bromooctyloxy)-[1,1'-biphenyl]-4-carboxylate, 6b .....	53
3.3.2(g)	Synthesis of 2-methylbutyl-4'-(bromononyloxy)-[1,1'-biphenyl]-4-carboxylate, 6c .....	53
3.3.2(h)	Synthesis of 2-methylbutyl-4'-(bromodecyloxy)-[1,1'-biphenyl]-4-carboxylate, 6d .....	53
3.3.2(i)	Synthesis of 2-methylbutyl-4'-(bromoundecyloxy)-[1,1'-biphenyl]-4-carboxylate, 6e .....	53
3.3.2(j)	Synthesis of 2-methylbutyl-4'-(bromododecyloxy)-[1,1'-biphenyl]-4-carboxylate, 6f.....	53

3.3.2(k)	Synthesis of 2-methylbutyl 4'-(azidoalkoxy)-[1,1'-biphenyl]-4-carboxylate, 7a-7f .....	54
3.3.2(l)	Synthesis of ( <i>E</i> )-2-methylbutyl-4'-((4-(((4'-cyano-[1,1'-biphenyl]-4-yl)imino)-2-ethoxyphenoxy)methyl)-1H-1,2,3-triazol-1-yl)alkoxy)-[1,1'-biphenyl]-4-carboxylate, 8aA–8fA .....	54
3.3.2(m)	Synthesis of ( <i>E</i> )-2-methylbutyl-4'-((4-((2-ethoxy-4-(((4-methoxyphenyl)imino)phenoxy)methyl)-1H-1,2,3-triazol-1-yl)alkoxy)-[1,1'-biphenyl]-4-carboxylate, 8aB – 8fB .....	55
<b>CHAPTER 4 RESULTS AND DISCUSSION.....</b>		<b>56</b>
4.1	Introduction .....	56
4.2	Bent-Monomeric Triazole-cored Liquid Crystals, 4aA – 4dA and 4aB – 4dB .....	56
4.2.1	Physical Properties .....	56
4.2.2	Fourier Transform Infrared (FTIR) Spectroscopy .....	58
4.2.3	Fourier Transform Nuclear Magnetic Resonance (FTNMR) Spectroscopy .....	62
4.2.4	Liquid Crystalline Behaviour from Differential Scanning Calorimetry (DSC) and Polarizing Optical Microscope (POM) .....	81
4.2.5	Computational Study by Density Functional Theory (DFT) .....	91
4.3	Bent-Dimeric Triazole-cored Liquid Crystals, 8aA – 8fA and 8aB – 8fB ....	99
4.3.1	Physical Properties .....	99
4.3.2	Fourier Transform Infrared (FTIR) Spectroscopy .....	100
4.3.3	Fourier Transform Nuclear Magnetic Resonance (FTNMR) Spectroscopy .....	104
4.3.4	Liquid Crystalline Behaviour from Differential Scanning Calorimetry (DSC) and Polarizing Optical Microscope (POM) .....	124
4.3.4(a)	Odd-and-Even Effect of Bent-Dimeric Liquid Crystals .....	138
4.3.4(b)	Entropy Effect.....	140
4.3.5	Computational Study by Density Functional Theory (DFT) .....	143

<b>CHAPTER 5</b>	<b>CONCLUSION AND FUTURE RECOMMENDATIONS....</b>	<b>151</b>
5.1	Conclusion.....	151
5.2	Recommendations for Future Research .....	154
<b>REFERENCES</b> .....		<b>155</b>
<b>LIST OF PUBLICATIONS</b>		



## LIST OF TABLES

	Page
Table 4.1      Physical properties, molecular formula, percentage of yield and percentages of C, H and N of homologous compounds <b>4aA – 4dA</b> and <b>4aB – 4dB</b> .....	57
Table 4.2      Absorption frequencies of FTIR of homologous compound homologous compounds <b>4aA – 4dA</b> and <b>4aB – 4dB</b> .....	59
Table 4.3 <sup>1</sup> H-NMR chemical shifts ( $\delta$ /ppm) of homologous compounds <b>4aA – 4dA</b> and <b>4aB – 4dB</b> .....	67
Table 4.4 <sup>1</sup> H- <sup>1</sup> H correlations as inferred from COSY experiments of <b>4dA</b> and <b>4dB</b> .....	69
Table 4.5 <sup>13</sup> C-NMR chemical shifts ( $\delta$ /ppm) of homologous compounds <b>4aA – 4dA</b> and <b>4aB – 4dB</b> .....	74
Table 4.6 <sup>1</sup> H- <sup>13</sup> C correlations as obtained from two dimensional HMQC and HMBC experiments of homologs <b>4dA</b> and <b>4dB</b> .....	80
Table 4.7      Phase transition temperatures and enthalpy of homologous compounds <b>4aA – 4dA</b> and <b>4aB – 4dB</b> .....	87
Table 4.8      Entropy value and dimensionless unit $\Delta S/R$ of homologous compounds <b>4aA – 4dA</b> and <b>4aB – 4dB</b> .....	89
Table 4.9      Summary of significant parameters from DFT calculation for <b>4aA – 4dA</b> and <b>4aB – 4dB</b> .....	91
Table 4.10      Physical properties, molecular formula, percentage yield and percentages of C, H and N of homologous compounds <b>8aA – 8fA</b> and <b>8aB – 8fB</b> .....	99
Table 4.11      Absorption frequencies of FTIR of homologous compounds <b>8aA – 8fA</b> and <b>8aB – 8fB</b> .....	101
Table 4.12 <sup>1</sup> H-NMR chemical shifts ( $\delta$ /ppm) of homologous compounds <b>8aA – 8fA</b> .....	109

Table 4.13	<sup>1</sup> H-NMR chemical shifts ( $\delta$ /ppm) of homologous compounds <b>8aB</b> – <b>8fB</b> .....	110
Table 4.14	<sup>1</sup> H- <sup>1</sup> H correlations as inferred from COSY experiments of <b>8dA</b> and <b>8dB</b> .....	112
Table 4.15	<sup>13</sup> C-NMR chemical shifts ( $\delta$ /ppm) of homologous compounds <b>8aA</b> – <b>8fA</b> and <b>8aB</b> – <b>8fB</b> .....	117
Table 4.16	<sup>1</sup> H- <sup>13</sup> C correlations as obtained from two dimensional HMQC and HMBC experiments of homologues <b>8dA</b> and <b>8dB</b> .....	123
Table 4.17	Phase transition temperatures and enthalpy ( $\text{kJmol}^{-1}$ ) of homologous compounds <b>8aA</b> – <b>8fA</b> and <b>8aB</b> – <b>8fB</b> .....	132
Table 4.18	Entropy values and dimensionless unit $\Delta S/R$ of homologous compounds <b>8aA</b> – <b>8fA</b> and <b>8aB</b> – <b>8fB</b> .....	140
Table 4.19	Summary of significant parameters from DFT calculation for <b>8aA</b> – <b>8fA</b> and <b>8aB</b> – <b>8fB</b> .....	146

## LIST OF FIGURES

	<b>Page</b>
Figure 1.1      General template of bent-shaped liquid crystal.....	3
Figure 1.2      Click reaction used to synthesize 1,4-disubstituted [1,2,3]-triazole ....	4
Figure 2.1      Illustration on molecular arrangements of a solid (left), liquid crystal (middle) and isotropic liquid (right) .....	11
Figure 2.2      Molecular structure of cholesteryl benzoate. ....	12
Figure 2.3      Stack up of different types of liquid crystals .....	14
Figure 2.4      General molecular template to design liquid crystalline molecule ....	16
Figure 2.5      Molecules consist of hydrophilic head and hydrophobic tail that form lyotropic liquid crystals .....	25
Figure 2.6      Molecular arrangements in liquid crystalline mesophases .....	26
Figure 2.7      Structure of a disc-like shaped molecule hexa(n-octyloxy)hexa- peri-hexabenzocoronene that commonly forms discotic liquid crystals.....	28
Figure 2.8      Phases and orientations of bent-shaped liquid crystals (BLCs).....	32
Figure 2.9      Schematic alignment of molecules along director, n, forming nematic phase and the commonly observed nematic Schlieren texture.....	35
Figure 2.10      Schematic packing of molecules in layers forming smectic A and smectic C phases .....	36
Figure 2.11      Optical photomicrograph of focal conic texture of SmA (left), and broken fan-shaped texture of SmC phase (right) .....	37
Figure 2.12      (From left to right) Schematic representation of rectangular and hexagonal columnar assembly and a typical texture of the hexagonal columnar phase .....	38

Figure 2.13	Optical photomicrograph showing mosaic pattern of B <sub>1</sub> phase and broken fan-shaped texture of B <sub>6</sub> phase.....	39
Figure 2.14	Molecular packing in adjacent layers of SmCP phases of Bent Liquid Crystal. (+) and (–) indicate the sign of layer chirality .....	40
Figure 3.1	Synthetic pathway to prepare ( <i>E</i> )-4'-((3-ethoxy-4-((1-alkyl-1H-1,2,3-triazol-4-yl)methoxy)benzylidene)-[1,1'-biphenyl]-4-carbonitrile, <b>4aA</b> – <b>4dA</b> .....	45
Figure 3.2	Synthetic pathway to prepare ( <i>E</i> )-4'-(3-ethoxy-4-((1-alkyl-1H-1,2,3-triazol-4-yl)methoxy)benzylidene)-4-methoxyphenyl, <b>4aB</b> – <b>4dB</b> .....	46
Figure 3.3	Synthetic pathway to prepare ( <i>E</i> )-2-methylbutyl-4'-((4-((4-(((4'-cyano-[1,1'-biphenyl]-4-yl)imino)-2-ethoxyphenoxy)methyl)-1H-1,2,3-triazol-1-yl)alkoxy)-[1,1'-biphenyl]-4-carboxylate, <b>8aA</b> – <b>8fA</b> .....	50
Figure 3.4	Synthetic pathway to prepare ( <i>E</i> )-2-methylbutyl-4'-((4-((2-ethoxy-4-(((4-methoxyphenyl)imino)phenoxy)methyl)-1H-1,2,3-triazol-1-yl)alkoxy)-[1,1'-biphenyl]-4-carboxylate, <b>8aB</b> – <b>8fB</b> .....	51
Figure 4.1	FTIR spectrum of representative compound <b>4dA</b> .....	60
Figure 4.2	FTIR spectrum of representative compound <b>4dB</b> .....	61
Figure 4.3	<sup>1</sup> H-NMR spectrum of representative compound <b>4dA</b> .....	65
Figure 4.4	<sup>1</sup> H-NMR spectrum of representative compound <b>4dB</b> .....	66
Figure 4.5	<sup>1</sup> H- <sup>1</sup> H COSY spectrum of representative compound <b>4dA</b> .....	68
Figure 4.6	<sup>1</sup> H- <sup>1</sup> H COSY spectrum of representative compound <b>4dB</b> .....	68
Figure 4.7	<sup>13</sup> C-NMR spectrum of representative compound <b>4dA</b> .....	72
Figure 4.8	<sup>13</sup> C-NMR spectrum of representative compound <b>4dB</b> .....	73
Figure 4.9	DEPT-90 spectrum of representative compound <b>4dA</b> .....	76
Figure 4.10	DEPT-90 spectrum of representative compound <b>4dB</b> .....	76
Figure 4.11	DEPT-135 spectrum of representative compound <b>4dA</b> .....	77
Figure 4.12	DEPT-135 spectrum of representative compound <b>4dB</b> .....	77

Figure 4.13	$^1\text{H}$ - $^{13}\text{C}$ HMQC spectrum of representative compound <b>4dA</b> .....	78
Figure 4.14	$^1\text{H}$ - $^{13}\text{C}$ HMBC spectrum of representative compound <b>4dA</b> .....	78
Figure 4.15	$^1\text{H}$ - $^{13}\text{C}$ HMQC spectrum of representative compound <b>4dB</b> .....	79
Figure 4.16	$^1\text{H}$ - $^{13}\text{C}$ HMBC spectrum of representative compound <b>4dB</b> .....	79
Figure 4.17	Optical photomicrograph during cooling cycle for compound <b>4cA</b> in which the four-fold closely packed fan-shaped texture of SmA phase with birefringence was observed at 127.0 °C .....	84
Figure 4.18	Optical photomicrographs showing focal conic fan-shaped texture of SmA phase, upon cooling for compound <b>4dA</b> at (a) 124.0 °C, and (b) 122.0 °C.....	84
Figure 4.19	Plot of clearing temperatures of homologous compounds <b>4aA</b> – <b>4dA</b> and <b>4aB</b> – <b>4dB</b> .....	87
Figure 4.20	DSC thermogram of compound <b>4dA</b> upon heating and cooling.....	88
Figure 4.21	DSC thermogram of compound <b>4dB</b> upon heating and cooling.....	88
Figure 4.22	Plot of dimensionless unit $\Delta S/R$ of homologous compounds <b>4aA</b> – <b>4dA</b> and <b>4aB</b> – <b>4dB</b> .....	90
Figure 4.23	Plot of $\Delta E$ of homologous compounds <b>4aA</b> – <b>4dA</b> and <b>4aB</b> – <b>4dB</b> ..	96
Figure 4.24	Plot of hardness, $\eta$ and softness, $\sigma$ of homologous compounds <b>4aA</b> – <b>4dA</b> and <b>4aB</b> – <b>4dB</b> .....	96
Figure 4.25	Plot of dipole moment of homologous compounds <b>4aA</b> – <b>4dA</b> and <b>4aB</b> – <b>4dB</b> .....	97
Figure 4.26	Surface charges of the optimized conformations for homologous compounds a) <b>4aA</b> , b) <b>4bA</b> , c) <b>4cA</b> and d) <b>4dA</b> . The atoms were represented in colours as follows: grey= C; red= O; blue= N .....	98
Figure 4.27	Surface charges of the optimized conformations for homologous compounds a) <b>4aB</b> , b) <b>4bB</b> , c) <b>4cB</b> and d) <b>4dB</b> . The atoms were represented in colours as follows: grey= C; red= O; blue= N .....	98
Figure 4.28	FTIR spectrum of representative compound <b>8dA</b> .....	102
Figure 4.29	FTIR spectrum of representative compound <b>8dB</b> .....	103

Figure 4.30	$^1\text{H}$ -NMR spectrum of representative compound <b>8dA</b> .....	107
Figure 4.31	$^1\text{H}$ -NMR spectrum of representative compound <b>8dB</b> .....	108
Figure 4.32	$^1\text{H}$ - $^1\text{H}$ COSY spectrum of representative compound <b>8dA</b> .....	111
Figure 4.33	$^1\text{H}$ - $^1\text{H}$ COSY spectrum of representative compound <b>8dB</b> .....	111
Figure 4.34	$^{13}\text{C}$ -NMR spectrum of representative compound <b>8dA</b> .....	115
Figure 4.35	$^{13}\text{C}$ -NMR spectrum of representative compound <b>8dB</b> .....	116
Figure 4.36	DEPT-90 spectrum of representative compound <b>8dA</b> .....	119
Figure 4.37	DEPT-90 spectrum of representative compound <b>8dB</b> .....	119
Figure 4.38	DEPT-135 spectrum of representative compound <b>8dA</b> .....	120
Figure 4.39	DEPT-135 spectrum of representative compound <b>8dB</b> .....	120
Figure 4.40	$^1\text{H}$ - $^{13}\text{C}$ HMQC spectrum of representative compound <b>8dA</b> .....	121
Figure 4.41	$^1\text{H}$ - $^{13}\text{C}$ HMBC spectrum of representative compound <b>8dA</b> .....	121
Figure 4.42	$^1\text{H}$ - $^{13}\text{C}$ HMQC spectrum of representative compound <b>8dB</b> .....	122
Figure 4.43	$^1\text{H}$ - $^{13}\text{C}$ HMBC spectrum of representative compound <b>8dB</b> .....	122
Figure 4.44	Optical photomicrographs showing the emergence of nematic texture and the disappearance of the texture when approaching isotropic liquid upon heating for compound <b>8bA</b> at (a) 117.0 °C, (b) 120.0 °C and (c) 128.0 °C.....	127
Figure 4.45	Optical photomicrographs showing two-fold and four-fold defect texture of nematic phase, upon cooling for compound <b>8bA</b> at (a) 114.0 °C, and (b) 119.5 °C.....	127
Figure 4.46	DSC thermograms of homologous compounds <b>8bA</b> and <b>8dA</b> .....	130
Figure 4.47	Phase sequence temperature ranges of <b>8aA</b> – <b>8fA</b> upon cooling.....	130
Figure 4.48	Optical photomicrographs showing two-fold and four-fold defect texture of nematic phase upon cooling for compound <b>8dA</b> at (a) 124.1 °C, nematic oily streak texture at (b) 115.3 °C, focal conic broken fan-shaped texture of anticlinic smectic C phase ( $\text{SmC}_a$ ) at	

	(c) 95.0 °C and (d) homeotropic dark conglomerate phase in the absence of birefringent appeared in circular motion at 88.0 °C .....	131
Figure 4.49	Optical photomicrographs showing (a) dendritic growth of Banana B <sub>1</sub> phase at 73.5 °C, and (b) mosaic texture, upon cooling of compound <b>8bB</b> .....	136
Figure 4.50	Optical photomicrographs showing Schlieren texture of SmC phase at (a) 66.5 °C, and (b) 63.4 °C, upon cooling of compound <b>8cB</b> .....	136
Figure 4.51	DSC thermogram of compound <b>8bB</b> during heating (red) and cooling (blue) cycle.....	137
Figure 4.52	Clearing temperatures of homologous compounds <b>8aA – 8fA</b> and <b>8aB – 8fB</b> as determined by DSC analysis .....	137
Figure 4.53	Transition temperatures versus length of alkyl chain during cooling cycle of homologous <b>8aA – 8fA</b> .....	139
Figure 4.54	Plot of dimensionless unit $\Delta S/R$ of homologous compounds <b>8aA – 8fA</b> and <b>8aB – 8fB</b> .....	141
Figure 4.55	Surface charges of the optimized conformations for homologue compounds (a) <b>8aA</b> , (b) <b>8bA</b> , (c) <b>8cA</b> , (d) <b>8dA</b> , (e) <b>8eA</b> and (f) <b>8fA</b> . The atoms were represented in the following colours: grey= C; red= O; blue= N.....	144
Figure 4.56	Surface charges of the optimized conformations for homologue compounds (a) <b>8aB</b> , (b) <b>8bB</b> , (c) <b>8cB</b> , (d) <b>8dB</b> , (e) <b>8eB</b> and (f) <b>8fB</b> . The atoms were represented in the following colours: grey= C; red= O; blue= N .....	145
Figure 4.57	Plot of $\Delta E$ of homologous compounds <b>8aA – 8fA</b> and <b>8aB – 8fB</b> ..	148
Figure 4.58	Plot of hardness, $\eta$ and softness, $\sigma$ of homologous compounds <b>8aA – 8fA</b> and <b>8aB – 8fB</b> .....	149
Figure 4.59	Plot of dipole moment of homologous compounds <b>8aA – 8fA</b> and <b>8aB – 8fB</b> .....	149

## LIST OF SYMBOLS

$\eta$	Chemical hardness
$\delta/\text{ppm}$	Chemical shift
$\sigma$	Chemical softness
$T_c$	Clearing temperature
$J$	Coupling constant
D	Debye
$^{\circ}\text{C}$	Degree Celsius
$\Delta S/R$	Dimensionless unit for entropy
eV	Electron Volt
$E_{\text{HOMO}}$	Energy at HOMO
$E_{\text{LUMO}}$	Energy at LUMO
$\Delta H$	Enthalpy
$\Delta H_C$	Enthalpy during clearing/isotropization
$\Delta H_N$	Enthalpy during nematic transition
$\Delta S$	Entropy
g	Gram
Ha	Hartree
$\Delta H_{I-N}$	Isotropic liquid to nematic phase enthalpy
$T_{I-N}$	Isotropic liquid to nematic phase transition temperature
$\text{JK}^{-1}$	Joule per Kelvin
$\text{kJmol}^{-1}$	Kilojoule per mol
MHz	Megahertz
mL	Milliliter
mmol	Millimole
$\Delta T_N$	Nematogenic temperature range



$\delta^-$	Partial negative
$\delta^+$	Partial positive
%	Percent
$\pi - \pi$	Pi to pi
P	Polarization
$^{\circ}\text{C}/\text{min}$	Rate (change in temperature per minute)
$\Delta T_{Sm}$	Smectogenic temperature range
%T	Transmission
$\delta_{\text{core}}$	Unit for cohesive energy density
$\nu/\text{cm}^{-1}$	Wavenumber/absorption frequency

## LIST OF ABBREVIATIONS

$C_nH_{2n+1}N_3$	1-azidoalkane
SmC <sub>a</sub>	Anticlinic Smectic C
SmC <sub>A</sub> P <sub>A</sub>	Anticlinic Smectic C with Antiferroelectricity
SmC <sub>A</sub> P <sub>F</sub>	Anticlinic Smectic C with Ferroelectricity
ATR	Attenuated Total Reflectance
B phase	Banana Phase
B3LYP	Becke, 3-Parameter, Lee–Yang–Parr
BLC	Bent-shaped Liquid Crystal
<sup>13</sup> C-NMR	Carbon Nuclear Magnetic Resonance
CHN	Carbon, Hydrogen and Nitrogen
N*	Chiral Nematic
SmA*	Chiral Smectic A
SmC*	Chiral Smectic C
CED	Cohesive Energy Density
CuSO <sub>4</sub> .5H <sub>2</sub> O	Copper (II) Sulphate Pentahydrate
COSY	Correlation Spectroscopy
Cr	Crystal
Cr <sub>1</sub>	Crystal 1
Cr <sub>2</sub>	Crystal 2
Cr <sub>3</sub>	Crystal 3
Cr <sup>[*]</sup>	Crystalline Phase composed of a Conglomerate Chiral Domain
CN	Cyano
DC	Dark Conglomerate
DFT	Density Functional Theory
CDCl <sub>3</sub>	Deuterated Chloroform
DCM	Dichloromethane
DSC	Differential Scanning Calorimetry
DMF	Dimethylformamide
DM	Dipole Moment
n(r)	Director
DEPT	Distortionless Enhancement by Polarization Transfer

-OC <sub>12</sub> H <sub>25</sub>	Dodecyloxy Terminal Chain
d	Doublet
EtOH	Ethanol
FTIR	Fourier Transform Infrared
FTNMR	Fourier Transform Nuclear Magnetic Resonance
HMBC	Heteronuclear Multiple Bond Correlation
HMQC	Heteronuclear Multiple Quantum Correlation
HOMO	Highest Occupied Molecular Orbital
I	Isotropic
LCD	Liquid Crystal Display
LUMO	Lowest Unoccupied Molecular Orbital
OCH <sub>3</sub>	Methoxy
m	Multiplet
N	Nematic
N <sub>D</sub>	Nematic Phase in Discotic Liquid Crystal
n	Number of Methylene Carbon
POM	Polarizing Optical Microscope
K <sub>2</sub> CO <sub>3</sub>	Potassium Carbonate
<sup>1</sup> H-NMR	Proton Nuclear Magnetic Resonance
q	Quartet
s	Singlet
Sm	Smectic
SmA	Smectic A
SmB	Smectic B
SmC	Smectic C
NaN <sub>3</sub>	Sodium Azide
SmC <sub>s</sub> P <sub>A</sub>	Synclinic Smectic C With Antiferroelectricity
SmC <sub>s</sub> P <sub>F</sub>	Synclinic Smectic C With Ferroelectricity
TMS	Tetramethylsilane
TLC	Thin Layer Chromatography
SmCP	Tilted Polar Smectic C
t	Triplet
N <sub>TB</sub>	Twisted Bend Nematic
TGB	Twisted Grain Boundary

2D	Two Dimensional
UV	Ultraviolet

**SINTESIS DAN SIFAT MESOMORFIK BES SCHIFF DENGAN  
KUMPULAN ETOKSI LATERAL PADA KEDUDUKAN 1,4-  
DITERTUKARGANTI BERTERASKAN TRIAZOL YANG BERBENTUK  
BENGKOK**

**ABSTRAK**

Dua siri molekul hablur cecair berbentuk bengkok, yang menggabungkan bes Schiff berteraskan teras triazol 1,4-ditertukarganti dengan kumpulan etoksi lateral, telah berjaya disintesis melalui tindak balas pensiklotambahan azida-alkuna yang menggunakan kuprum sebagai mangkin. Pencirian molekul dijalankan menggunakan teknik spektroskopik, manakala mikroskop optik polarisasi (POM) dan kalorimetri pengimbasan pembezaan (DSC) digunakan untuk mengkaji sifat optik dan termal molekul. Dalam siri pertama, molekul direka bentuk sebagai sebatian monomer bengkok ringkas yang mengandungi bes Schiff etoksi lateral dengan rantai alkil fleksibel terminal, dengan panjang rantai yang berbeza. Subsiri A dengan zat penukarganti bes Schiff yang bersambung kepada sianobifenil pada kedudukan terminal mempamerkan fasa SmA yang stabil bagi sebatian dengan rantai alkil yang lebih panjang. Hal ini lantas menunjukkan bahawa sifat smektogenik dipengaruhi oleh fleksibiliti molekul melalui pemanjangan rantai. Sebaliknya, semua terbitan subsiri B dengan zat penukarganti bes Schiff yang bersambung kepada fenil metoksi menunjukkan ketiadaan sifat mesomorfik dengan penyejukan berlebihan yang ketara. Manakala, siri kedua yang menunjukkan ciri mesofasa berbeza dan lebih jelas telah dibentuk beranalog siri pertama sebagai sebatian dimer berteraskan triazol yang dihubungkan kepada penghalang alkoksi dengan ester bifenil pada satu sisi. Kesan ketara pengubahsuaian struktur ini dapat dilihat ke atas sifat mesomorfik sebatian.

Semua derivatif dalam subsiri A mempamerkan watak nematogenik dengan tekstur Schlieren dwirefringen. Sebatian **8bA** mempamerkan tingkah laku enantiotropik dengan keadaan berkaca apabila disejukkan, manakala **8dA** menunjukkan fasa nematik berminyak yang berjalur dan tekstur smectik frustrasi yang menarik. Derivatif subsiri B secara amnya tidak mempunyai sifat mesogenik yang jelas. Semasa penyejukan, hanya homolog **8bB** dan **8cB** yang memaparkan fasa B<sub>1</sub> dan fasa SmC Schlieren. Teori Ketumpatan Fungsi (DFT) yang digunakan bagi menyelidik konformasi struktur dan pengaruh momen dwikutub ke atas sifat mesofasa homolog **4aA – 4dA**, **4aB – 4dB**, **8aA – 8fA** dan **8aB – 8fB** telah mendedahkan pengaruh peningkatan momen dipol dan konformasi molekul optimum dalam menstabilkan mesofasa tercerap. Penemuan ini memberikan pemahaman yang lebih mendalam tentang bagaimana struktur molekul mempengaruhi tingkah laku dinamik dan kestabilan fasa hablur cecair.

# SYNTHESIS AND MESOMORPHIC PROPERTIES OF BENT-SHAPED 1,4-DISUBSTITUTED TRIAZOLE-CORED SCHIFF BASE WITH LATERAL ETHOXY GROUP

## ABSTRACT

Two series of bent-shaped liquid crystalline molecules, incorporating 1,4-disubstituted triazole-cored Schiff bases with lateral ethoxy groups, were successfully synthesized via the copper-catalyzed azide-alkyne cycloaddition reaction. Molecular elucidation was conducted using spectroscopic techniques, while polarizing optical microscopy (POM) and differential scanning calorimetry (DSC) were employed to investigate the optical and thermal properties of the molecules. In the first series, molecules were designed as simple bent monomers containing lateral ethoxy Schiff base with terminal flexible alkyl chains of varying lengths. Subseries A consists of cyanobiphenyl Schiff base at terminal position, exhibited stable SmA phases in compounds with longer alkyl chains, suggesting that an increase in molecular flexibility with chain lengthening favours smectogenic character. In contrast, all derivatives of subseries B with phenyl methoxy Schiff base at terminal position showed non-mesomorphic behaviour with significant overcooling tendencies. The second series, which is analogous to the first but extending into a dimer with a triazole core and an alkoxy spacer linked to a biphenyl ester on one side, displayed more distinct and pronounced mesophase characteristics. This demonstrates the significant impact of these structural modification on mesomorphic properties. All derivatives in subseries A, **8aA** – **8fA** exhibited nematogenic character with birefringent Schlieren texture. Notably, homologue **8bA** is the only derivative showcasing enantiotropic behavior with a glassy state upon cooling, while **8dA** revealed an intriguing striated

oily nematic and frustrated smectic phase. Subseries B derivatives generally lacked mesogenic properties. Only homologues **8bB** and **8cB** displayed the B<sub>1</sub> phase and Schlieren SmC phase, respectively, during cooling. The investigation into the structural conformation and the influence of dipole moments on mesophase properties of homologous **4aA – 4dA**, **4aB – 4dB**, **8aA – 8fA** and **8aB – 8fB** using Density Functional Theory (DFT) revealed that increased dipole moments and optimal molecular conformations are critical in stabilizing the observed mesophases. These findings offer a deeper understanding of how molecular structure directly influences the dynamic behaviour and phase stability of these liquid crystals.



# CHAPTER 1

## INTRODUCTION

### 1.1 Overview

Liquid crystals (LCs) are unique materials that exhibit properties between those of conventional liquids and solid crystals. These phases offer remarkable versatility and have become essential in advanced materials and technologies. Bent-shaped liquid crystals (BLCs) that are characterized by their bent or banana-shaped molecular geometry, exhibit a range of complex phases, including smectic, biaxial nematic, and ferroelectric phases. The molecules' bent shape causes them to align and interact with external fields in a unique way, and this is what gives the liquid crystal phases their special optical and electro-optical characteristics (Matsuyama, 2020). The incorporation of heterocyclic core often leads to the enhancement of thermal and chemical stability, hence expanding the range of potential applications (Gallardo et al., 2012). Liquid crystals with a [1,2,3]-triazole core are ought to offer a different set of advantages due to the stability and functional versatility imparted towards the overall liquid crystalline system.

### 1.2 Bent-shaped/Banana-shaped Liquid Crystals (BLCs)

Bent-shaped liquid crystals (BLCs), also known as banana-shaped liquid crystals, are a unique class of liquid crystalline materials distinguished by their molecular shape, which resembles a bent or banana-like structure (Kang et al., 2006). This distinctive geometry leads to a variety of complex and intriguing behaviours not observed in conventional rod-like or discotic liquid crystals. BLCs exhibit a wide range of phases, from nematic phases to various frustrated liquid crystalline phases including banana phases with unique optical, electro-optical, and viscoelastic

properties. These properties make BLCs particularly valuable for advanced applications in display technologies, sensors, photonic devices, and smart materials (Teng et al., 2011).

The discovery of bent or banana-shaped liquid crystals dates back nearly three decades. This breakthrough opened up a new area of research in liquid crystal science, revealing properties and phases not observed in traditional liquid crystals (Berladean et al., 2023). Bent-shaped liquid crystalline molecules have captured researchers' attention due to their self-assembly properties, which lead to the generation of polar ordering and the attainment of chirality even in achiral molecules (Alaasar et al., 2019). These characteristics are particularly noteworthy because they enable spontaneous ferroelectric order, which holds significant potential for advanced technological applications (Hird, 2011).

This thermotropic-type liquid crystal has been studied for its mesomorphism and behaviours by incorporating numerous bent-core units, contributing to its bent shape. Various mesogenic cores such as benzene core (Alaasar, 2016), [1,2,4]-oxadiazole (Shanker et al., 2014), [3,5]-pyrazole (Hariprasad & Srinivasa, 2015) and [1,2,3]-triazole (Wang et al., 2019) have been utilized as the deviation point accompanied by a bending angle, to design liquid crystalline molecules with bent conformation. Considering the bent-shaped molecule is a dynamic system as depicted in Figure 1.1, even a slight structural modification can result in different physical properties. The central aromatic unit plays a crucial role in stabilizing mesomorphic behaviour through the  $\pi$ - $\pi$  interactions (Kovářová et al., 2014). It is worth mentioning that Majumdar et al. (2011) has reported the two arms linked to the oxadiazole unit are angled relative to each other, giving an overall bent shape to the molecule. This

structural arrangement potentially enhances flexoelectric contributions, leading to large thermal ranges appearance of chiral frustrated phases.

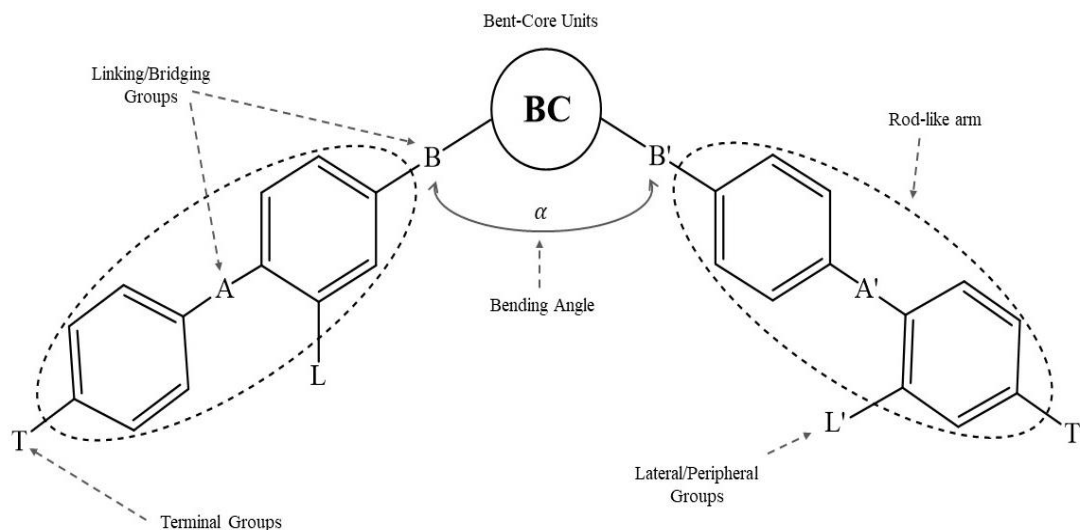


Figure 1.1 General template of bent-shaped liquid crystal (Scutaru et al., 2019)

The packing of bent-shaped molecules, which can be more or less rigid with long terminal chains, induces an optimal distribution of electronic density throughout the molecules, stimulating mesomorphism (Panarin et al., 2020). The peripheral core substitution is also found to favour polar order in bent-shaped liquid crystals (Alaasar et al., 2017). Moreover, Ciobanu et al. (2021) has also reported the synthesis of bent-shaped liquid crystalline molecules incorporating the bent-core isophthalic derivatives that showcased the appearance of transition from nematic (N) phase with Schlieren and ribbon textures to focal conic smectic phase upon cooling for alkyl chain  $n=7$ . They also investigated the molecular modelling for polar packing with ferroelectric and antiferroelectric order. Building on these findings, the incorporation of diverse molecular cores, has further expanded the potential for designing liquid crystals with tailored mesomorphic properties and enhanced polar order.

### 1.3 Liquid Crystalline Compounds with [1,2,3]-Triazole Core

One of the prevalent groups within the bent-core systems is associated with the five-membered ring, such as the [1,2,3]-triazole. The triazole moiety is formed through a [2, 3]-dipolar cycloaddition reaction between an organic azide and a terminal alkyne, known as the 'click reaction' as demonstrated in Figure 1.2. This versatile chemistry has attracted considerable attention in various scientific fields, including materials chemistry, organic chemistry, supramolecular chemistry, drug discovery, and bio-conjugation (Balamurugan et al., 2012; Fang et al., 2021; Xia et al., 2021).

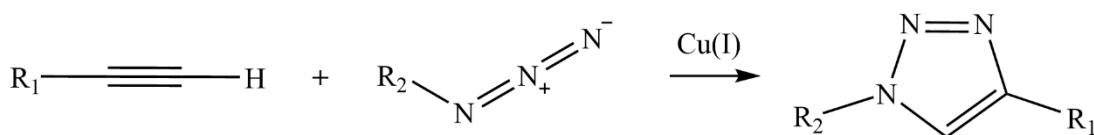


Figure 1.2 Click reaction used to synthesize 1,4-disubstituted [1,2,3]-triazole (Ramapanicker & Chauhan, 2016).

The inclusion of nitrogen atoms within the triazole rigid core generally acts as a dipole within the molecule, serving multiple purposes, such as i) generating a force that induces tilting, ii) disrupting the inversion centre of symmetry, and iii) amplifying the transverse dipole moment in the molecule (Balamurugan et al., 2014; Rodrigues et al., 2020). As such, the nitrogen atom plays a pivotal role in improving the self-ordering of mesogenic phases. Furthermore, the emergence of smectic C phase is influenced by the molecular packing, where the long axis of the molecules tilts about the normal plane, resulting in biaxiality (Heng et al., 2014). In contrast, molecules in the smectic A phase align parallelly, with their long axes perpendicular to the planes, exhibiting uniaxiality.

A series of bent luminescent (benzothiadiazolyl)triazole (BTT) derivatives was synthesized using click chemistry by de Oliveira Costa et al. (2024). Two

representative compounds, 7b and 7f, featuring 4-alkoxyarylethynyl and 2-alkoxynaphthylethynyl substituents, respectively, displayed smectic C mesomorphism during both heating and cooling cycles, as elongated batonnets textures coalesced to form the broken fan texture of SmC. This behavior is likely attributed to an increase in molecular dipole and dielectric anisotropy, resulting in polar organization at the intermolecular level (Paterson et al., 2023).

Moreover, the triazole core's electron-rich nature and its ability to participate in hydrogen bonding interactions contribute to the formation of unique supramolecular structures within liquid crystal phases. These interactions are particularly beneficial in stabilizing mesophases, which are otherwise prone to destabilization due to the inherent flexibility of the liquid crystal molecules (Xia et al., 2021). As a result, triazole-based liquid crystals have been shown to exhibit a wide variety of mesophases, including nematic, smectic, and columnar phases, making them versatile candidates for advanced material applications.

The strategic placement of the [1,2,3]-triazole aromatic ring in a central core position has given prominence to its beneficial properties, including lowering the melting point of molecules, increasing molecular dipole and dielectric anisotropy, as well as inducing molecular-level polar organizations through electrostatic and shape-dependent intermolecular interactions, favouring mesogenic phases (Li et al., 2017; Yeap et al., 2015).

#### **1.4 Problem Statement**

Liquid crystals (LCs) have been extensively studied, particularly the rod-like types, which are known for their well-defined mesomorphic properties and stable phase behaviour. These calamitic LCs have laid the groundwork for understanding the

fundamental principles of liquid crystal science. Meanwhile, bent-shaped liquid crystals (BLCs) are relatively new and have garnered significant scientific interest due to their distinct mesophase behaviors and potential applications (Scutaru et al., 2019).

However, despite extensive research in recent years, many aspects of BLCs remain unexplored, particularly concerning their monomers and extended dimers (Gak Simić et al., 2021; Paterson et al., 2017). The synthesis of molecules with varied alkyl chain configurations is essential to understanding their impact on mesophase behavior. The placement of flexible alkyl chains, whether at terminal positions or as inner spacers, significantly influences structural variations, charge distribution and the resulting mesophase (Sreenilayam et al., 2017).

The inherent deviation of BLCs from linearity introduces challenges, such as poor mesophase stability, which is often exacerbated by enhanced excluded volume during molecular rotation, leading to unpredictable phase behavior (Antal Jáklí & Lavrentovich, 2023). This issue may be mitigated by incorporating lateral substituents such as ethoxy group to fill the void left by molecular rotation. The inclusion of a 1,4-disubstituted triazole unit at the core position also can maintain the calamitic characteristics of liquid crystalline molecules, even within a bent conformation, thereby enhancing mesomorphism.

Stability and rigidity within BLC structures present additional problems. The [1,2,3]-triazole core introduces unique electronic properties and rigidity, which may stabilize the mesophase. Additionally, incorporating various components such as linking groups, and lateral or terminal substituents broadens the functionality of BLCs. Systematically investigating how these peripheral and terminal groups affect stability

and mesophase behavior is crucial for developing new liquid crystal textures (Mohiuddin et al., 2017).

Another significant challenge lies in exploring single-molecule reactivity, including molecular orbitals, dipole moments, and electron density, to understand how these factors influence the macroscopic properties of BLCs. To address this, a combined approach of computational studies using Density Functional Theory (DFT), and experimental data will be employed. This methodology aims to provide deeper insights into structure-property relationships through the analysis of HOMO-LUMO gaps, dipole moments, and surface charges at the molecular level.

## **1.5 Objectives**

The research objectives for this study are as follows:

1. To synthesize and characterize series of bent-shaped liquid crystalline monomers and dimers comprising of triazole core, flexible aliphatic chain at terminal or inner spacer and laterally ethoxy Schiff base with different terminal aromatic system using spectroscopic methods as well as thermal and optical analyses.
2. To evaluate the influence of varying length of alkyl chain and terminal substituents as well as the effect of alkoxy biphenyl carboxylate unit incorporation, forming dimer-type liquid crystalline compounds towards their mesophasic assemblies.
3. To predict the structure-property relationship based on the HOMO-LUMO energy gap, dipole moment and molecular conformations of homologous compounds by computational study using Density Functional Theory (DFT).

## 1.6 Research Scope

The scope of present study will be centred around the synthesis of two series of liquid crystalline compounds incorporating [1,2,3]-triazole as the mesogenic core, connected to a trisubstituted phenyl ring containing peripheral ethoxy group and a Schiff base. Each series will comprise of two different terminal substituents linked to the Schiff base in one side of triazole core, namely cyanobiphenyl and phenyl methoxy groups, respectively. The difference between these two series lies in the other side arm of the triazole mesogenic core.

The first series includes only terminal flexible carbon chain with  $n=9, 11, 12$  and  $16$  and they can be considered as monomeric liquid crystalline compounds. Meanwhile, for the second series, the flexible alkyl chain was introduced as a spacer, where more functional components are being added to the chain, therefore can be claimed as dimeric liquid crystalline materials. In this series, ester-biphenyl moiety was incorporated to the terminal end of the alkoxy chain with  $n=7 - 12$ , fabricating the molecule to adapt to a whole new conformation and behaviour.

The molecular structures of the synthesized compounds were elucidated using various spectroscopic techniques such as elemental analysis, Fourier Transform Infrared (FTIR) and Nuclear Magnetic Resonance (NMR). The texture observation was conducted utilizing Polarizing Optical Microscope (POM) with heating and cooling stage. Meanwhile, for thermal analysis, Differential Scanning Calorimetry (DSC) was employed to analyse the associated enthalpy and transition temperatures of the corresponding liquid crystalline materials. Furthermore, computational study by using Density Functional Theory (DFT) was integrated in analysing the compounds to the molecular level and identifying different electronic properties such as HOMO,



LUMO and the associated HOMO-LUMO gaps as well as dipole moments. The data obtained were then compared and correlated with the liquid crystalline behaviours of the respective compounds.

## **CHAPTER 2**

### **LITERATURE REVIEW**

#### **2.1 State of Matter**

Matter may be classified into numerous states or phases, including solid, liquid, and gas, which are referred to as the fundamental states of matter. Historically, states of matter were defined by qualitative differences in bulk properties. Solid is the condition in which matter keeps a constant volume and shape, liquid is the state in which matter adapts to the shape of its container but changes only slightly in volume, and gas is the state in which matter expands to occupy the volume and shape of its container. Each of these three classical states of matter can instantly transition into one another classical states (Dierking & Al-Zangana, 2017). Despite these renown states of matter, some materials existed could not be identified whether they belong to specific states of matter. Thus, as for materials in states of matter that are neither simple liquids nor crystalline solids, they are readily termed as soft condensed matter or simply soft matter (Bai & Liu, 2013) .

The idea of a unified approach to ‘soft materials/matter’ has only gained ground recently. Many such materials are familiar in everyday life-glues, paints, and soaps, while others, such as the polymer melts that are moulded and squeezed, are important in industrial processes to form plastics. Much of the food we eat can also be regarded as soft matter/soft material and indeed the stuff of life itself shares the qualities of mutability and responsiveness to its surroundings which are the characteristics of soft materials (Jones, 2002).

The term ‘soft’ matter originates from macroscopic mechanical properties. Materials such as colloids, surfactants, liquid crystals, specific biomaterials, and

polymers are classified as soft materials and can be induced to flow under certain conditions. This weak ordering results from a crystalline solid's lack of three-dimensional atomic long-range order. Nevertheless, there is always a degree of local order at least as great as that in a liquid (Hamley, 2007).

## 2.2 Introduction to Liquid Crystals

Everyday experience has led to universal familiarities with substances that undergo a single transition from solid to isotropic liquid phase. The melting of ice at 0°C to form liquid water is perhaps the most common displaying such phase transition. There are, however, many organic materials exuding several diverse intermediate phases that are said to be soft materials. Among previously mentioned soft materials, liquid crystal is a unique material in which displaying the stated properties (Goodby et al., 2015).



Figure 2.1 Illustration on molecular arrangements of a solid (left), liquid crystal (middle) and isotropic liquid (right) (Silbey, 1987).

The scientific term liquid crystal defines its own characteristics to flow like a liquid, but at the same time possess an orientational and even in some cases –positional order, which is the traits of solid crystals. Thus, it is not surprising that the molecular ordering in these intermediate phases, known as “mesophase”, lies between a three

dimensionally ordered crystalline solid state and the isotropic liquid exhibiting constant vector magnitude as illustrated in Figure 2.1.

The partially ordered, anisotropic fluids, and the intermediary state liquid crystal, was conventionally discovered backdated to year 1888 by the Austrian botanist Friedrich Reinitzer, who had uncovered two distinctive melting points observation in cholesterol-based compounds such as cholesteryl benzoate (Figure 2.2) and cholesteryl acetate. In between these two melting points, he observed that there was a milky liquid phase, while beyond the second melting, a clearer phase was observed (Mitov, 2014).

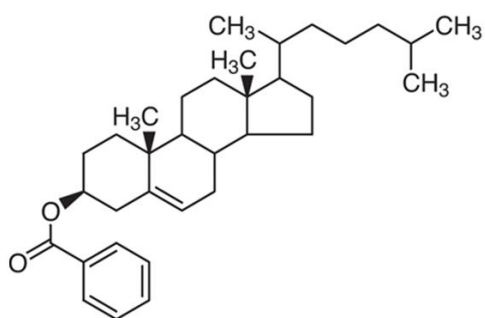


Figure 2.2 Molecular structure of cholesteryl benzoate.

Without really being able to explain the impact of his discovery, Reinitzer nevertheless realized that the discerned behaviour of the compounds he investigated was far different from the generally accepted view on the states of matter during his time. This should not detract from the fact that liquid crystalline phases might have been come across before, but the fundamental realization of a novel behaviour of matter was missing from those reports. Hence for further evaluation, Reinitzer contacted physicist Otto Lehmann, who owned a polarizing microscope with a hot stage that enabled them to study the phenomenon more precisely. Therefore, biologist Friedrich Reinitzer was considered as the pioneer discoverer of liquid crystal while Lehmann, the physicist, is

hailed as the founder of liquid crystal research (Bremer et al., 2013; Geelhaar et al., 2013).

Liquid crystals are widely recognized as partially ordered anisotropic fluids, occupying a transitional state between the highly ordered solid crystal and liquid phases. Their distinguishing features include orientational and low-dimensional positional order along the long molecular axis (Singh & Collings, 2003). Despite sharing an orientation characteristic with crystalline solids, liquid crystals possess the flow-like properties that enable them to be developed into liquid crystal displays (LCDs) (Mitov, 2014). The incorporation of liquid crystalline units in LCDs has significantly advanced technology, finding applications in modern electronic devices such as smartphones, flat-panel screen televisions, and portable computers (Wei et al., 2008). This historical and technological journey underscores the crucial role played by liquid crystals in shaping contemporary electronic display technologies (Kirsch & Bremer, 2010).

Liquid crystal can be classified into two major categories, namely the thermotropic liquid crystals and the lyotropic liquid crystals. The mesogens may exhibit several liquid crystal phases, which can be distinguished by the degree of order of the liquid crystalline molecules and their shapes, which comprised of three main groups: (a) calamitic (rod-like), (b) discotic (disc-like), and (c) bent-shaped (banana-like) liquid crystals as illustrated in Figure 2.3 (Carlescu, 2019).

A basic query that will be discussed many times in numerous ways is why some molecules form liquid crystalline phases or ordered fluid phases. How do molecules pack together without leaving much free volume/space between molecules is the central criterion that has always been the question. Molecular interactions are also important, with the polarity of the molecules important to the nature of these interactions. The

molecular entities that form liquid crystals can be quite complex, in whatever cases, the packing considerations become even more important, especially since complex molecular architectures allow for different and sometimes intricate packing structures (Jákli et al., 2018).

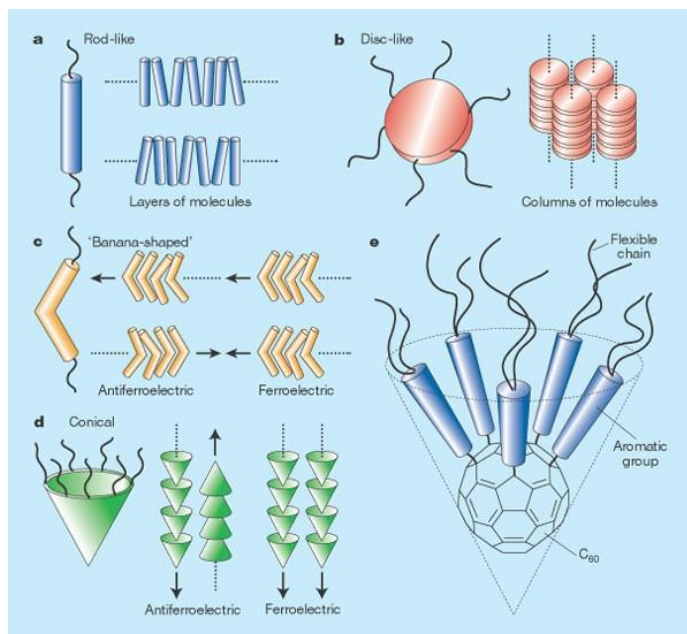


Figure 2.3 Stack up of different types of liquid crystals (Tschierske, 2002).

An example of the extreme complexity is when assemblies that were made by weakly interactions, bonded molecules together, thus forming the entities that possess orientational and/or positional order. It must be mentioned here also that such systems are extremely dynamic (Etxebarria & Ros, 2008). Obviously, positional order can be realized regardless of molecular shape, whereas orientational order has meaning only when the constituent molecules are non-spherical or elongated (Goodby et al., 2015). Thus, there is good reason to expect molecular structure to be an important factor in determining the kind and extent of ordering in any mesophase.

### **2.3 Molecular Building Blocks/Liquid Crystal Constituents**

Developing inexpensive novel liquid crystalline materials that possess both excellent thermal stability and a broad mesophase temperature range remains a persistent challenge. Nevertheless, one of the most effective approaches to address this challenge has been the strategic alteration of molecular geometries (Khoo, 2022). This method has proven highly efficient in the development of innovative, cost-effective liquid crystal materials with specific attributes. Even subtle adjustments to the molecular shape, such as introducing heteroatoms or employing various lateral substituted atoms or groups, can induce significant transformations in liquid crystalline properties, molecular geometry, transition temperature, conformational preferences, and other essential physical characteristics (Lintuvuori et al., 2018). These modifications are crucial for designing and producing new, economically viable liquid crystal materials with enhanced properties tailored for applications in display technologies.

In the pursuit of addressing this challenge, it is essential to incorporate specific molecular architectures and designs to attain the desired liquid crystalline characteristics, establishing the structure–property dependency. The fundamental conditions for a molecule to demonstrate liquid crystalline behaviour include i) elongated shape wherein the length exceeds its width, ii) rigid central part or core and iii) flexible chain incorporation. The self-aggregation in liquid crystals arises from the preferred molecular packing because of the strong intermolecular attractions (Wilson et al., 2022). The molecular design, crucial for inducing liquid crystalline behaviour, primarily involves the integration of constituents as illustrated in Figure 2.4, namely mesogenic cores, linking structures, terminal, and lateral groups, which encompasses a spectrum from polar substituents to bulky groups and flexible peripheral chains.

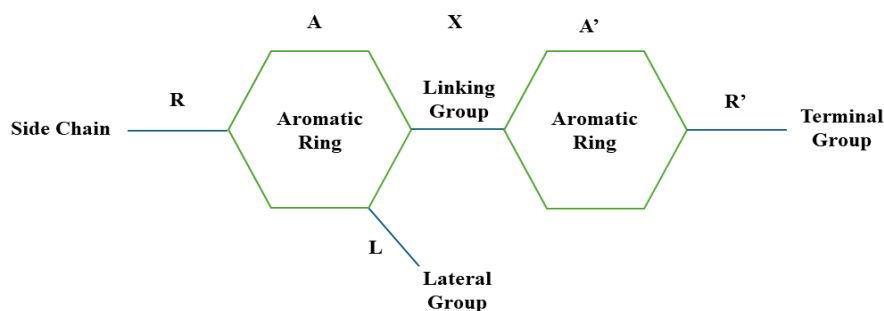


Figure 2.4 General molecular template to design liquid crystalline molecule.

### 2.3.1 Mesogenic Core

It is always important that the molecule is relatively rigid for at least some portion of its length. This property is designed to maintain an elongated shape to produce interactions that favour alignment and packing in an ordered way. The incorporation of two or more rigid ring structures is essential to establish stability and balance between fluidity and rigidity in fabricating liquid crystalline molecules with lower phase transition temperatures (Dierking, 2022).

Most liquid crystals are commonly made up of benzene rings; thus, they are benzene derivatives. Heterocyclic liquid crystals share structural similarities with benzene derivatives, replacing one or more benzene rings with groups like pyridine, pyrimidine, or equivalents. In diverse combinations, these may also encompass saturated cyclohexane or unsaturated phenyl, and biphenyl moieties (Goodby & Cowling, 2022). Among them, cholesterol derivatives are the pioneer and the most prevalent compounds demonstrating the cholesteric phase in liquid crystals (Ferrer-Ugalde et al., 2021).

Recently, biphenyl moiety has shown significant performance in the field of liquid crystal due to its polymer ability especially when coupled with terminal nitrile



group to readily exhibit nematic phase even in room temperature (Park et al., 2006; Zhang et al., 2020). It has attracted considerable attention from researchers due to its contribution in providing photochemical stability to liquid crystalline molecules. This feature enabling liquid crystal to display distinct texture of mesophase and widely nematic phases as well as smectic phases depending on the molecular conformation (Ha et al., 2010).

On the other hand, the incorporation of different mesogenic cores will result in distinct liquid crystalline conformations. Notably, the insertion of heterocyclic rings especially could induce bent conformations as well as high molecular dipole provided by negatively charged heteroatoms, thus contributes to the enhancement of liquid crystalline behaviour of molecules.

### **2.3.2 Flexible Chain**

Liquid crystals predominantly consist of organic molecules featuring  $\pi$ -conjugated systems and flexible alkyl chains. While the functional conjugated units play a critical role in maintaining order within the liquid crystal phase, their limited solubility in organic solvents poses significant challenges for processing in optoelectronic devices (Moonen et al., 2012). The attachment of alkyl chains is crucial in overcoming this limitation, as it not only enhances solubility but also lowers the melting points and protects the conjugated units from oxygen-related degradation. Achieving an optimal balance between the van der Waals interactions of alkyl chains and the  $\pi$ - $\pi$  interactions of conjugated units is pivotal in modulating the physical states of liquid crystals, thereby optimizing their optoelectronic properties (Lu & Nakanishi, 2015).

Sorai and Saito (2003) highlighted that the disordering of alkyl chains can lead to a significant entropy gain of approximately  $10 \text{ JK}^{-1}$  per mol of  $\text{CH}_2$  units, which

substantially influences the thermodynamic stability of the aggregated states in liquid crystals. These flexible chains, with their high mobility, act similarly to solvents within the liquid crystal matrix, impacting the phase behaviour and stability of the material. Meanwhile, Tschierske (2014) demonstrated that altering transition temperatures within a system by exchanging flexible peripheral chains is an effective method for modulating the entropic properties of liquid crystals. This approach underscores the importance of chain structure, as varying chain length, saturation, and branching can significantly affect the mesomorphic behaviour and stability of the resulting liquid crystal phase.

### **2.3.3 Linking Group**

A mesogen often consists of mesogenic core, flexible chain as well as lateral and terminal substituents. The core provides the necessary rigidity for anisotropy, while the flexible chain imparts stability to uphold molecular alignment in the mesophase (Kumar & Pal, 2018c). Commonly, the core of a mesogenic molecule is an aromatic ring, which is linearly linked either directly or through connecting units such as ester, azomethine, azo, stilbene, thiocarbonyl, or acryloyloxy types. The choice of linking groups significantly impacts chemical structures. The electronic nature of withdrawing or donating groups strongly influences electronic density, molecular flexibility, and the partial polarity within the molecule (Al-Zahrani et al., 2021).

Linking groups, usually, are characterized by simple bonds or groups. When utilized as linking groups in liquid crystalline molecules, the Schiff base linker groups offer various advantages. They are easily synthesized and adaptable to a variety of mesogenic architectures. The imine bond within Schiff bases is reasonably stable, contributing to the overall stability of the liquid crystal phase across a broad temperature range (Mohammady et al., 2022).

Schiff bases are often conjugated with benzene rings to elongate and enhance the compound's polarizability, thereby augmenting its liquid crystal behaviour. The Schiff base linkage introduces a stepped core structure, preserving molecular linearity and providing significant stability. Consequently, it induces mesophase development, with the connecting group influencing phase transition temperatures and physical characteristics of molecules (Ahmed et al., 2019).

In line with this, Ahmad et al., has also reported molecules with an ester linkage that were prepared in addition to Schiff base bridging group to increase the rotation of bent molecules and enhance the generation of conventional liquid crystalline phases. The incorporation of -CH=N- linkages to rigid phenyl rings provides a stepped core shape and helps retaining the linearity of the molecular structure. This enhancement thus contributes to the stability of formed mesophases (Ahmed et al., 2020). Furthermore, the dimers with ester or ether moieties often show the odd-and-even effect on the phase transition and the associated entropy changes when the length and parity of the spacer were varied (Arakawa et al., 2022).

#### **2.3.4 Terminal Group**

Enhancing the polarizability and polarity of the entire mesogenic molecule generally contributes to the improvement of its mesophase stability. The terminal group could be derived from either flexible chain, typically straight alkyl or alkoxy chains, as well as polar substituents. Depending on the type and composition of these substituents, a calamitic molecule can form either nematic or smectic mesophases. Substituents with different polarities positioned at both terminals along the molecular axis of a mesogenic compound have been observed to either promote or suppress mesophase thermal transitions. The high dipole moment which arose from polar substituent attachments, is

one of the probable factors that leads to the enhancement of lattice stability (Khan et al., 2018).

The dipole moments of individual components are normally influenced by the nature of substituents, as the mesophase stability of a liquid crystalline compound relies heavily on intermolecular attractions where molecular polarity plays a significant role. Terminal units such as cyano/nitrile groups favour the formation of liquid crystalline phases, due to the polar attractive interactions between pairs of adjacent molecules. The extent of conjugation affects the polarizability of the molecule and consequently alters its resulting dipole moment (Lu & Nakanishi, 2015; Naoum & Ahmed, 2011). Selvarasu and Kannan (2015) explored the impact of terminal substituents CN, Cl, H, CH<sub>3</sub>, and OCH<sub>3</sub> on the mesomorphism of azobenzene derivatives capped with cinnamoyl esters in their studies. Their findings revealed a broader transition temperature range in homologues with CN and Cl compared to other substituents. This suggests that the electron-withdrawing effect of CN and Cl homogenizes the strong  $\pi - \pi$  interaction across the molecules, implying a significant contribution to intermolecular and dipole-induced dipole interactions.

### **2.3.5 Lateral Group**

Lateral substituents also play a crucial role in controlling molecular packing. Literatures have extensively documented the introduction of a lateral group into the aromatic ring of a mesogenic core, which demonstrates a significant influence on the transition temperature range of smectic phases and enhances spontaneous polarization. The dipole moment of the entire compound depends primarily on the position and polarity of the attached lateral and terminal groups; thus, these moieties play an essential

role in the observed melting temperatures of the synthesized derivatives (Al-Zahrani et al., 2021).

Lateral substitution exerts a profound impact on the liquid crystalline state and mesophase stability. The packing of molecules is influenced by factors such as size, polarity, and substituent position. The introduction of bulky lateral substituents may lead to the complete disappearance of liquid crystalline properties. Conversely, the incorporation of small polar substituents sometimes results in interesting modifications in the switching behaviour. Recent investigations by Tun Nur Iskandar et al. (2020) revealed that liquid crystalline compounds containing trisubstituted phenyl derivatives with a lateral ethoxy group exhibit magnetic interactions which highlighted an exceptional phenomenon occurred from organic materials. Likewise, perhaps the most fundamental influence of lateral substitution is to generate the tilted smectic C phase by establishing a lateral dipole. This is especially crucial in the chiral smectic C phase that is the foundation of the ferroelectric displays (Naoum et al., 2015; Thakor et al., 2022).

#### **2.3.6 Triazole Core in Liquid Crystals**

The incorporation of heterocyclic units such as triazoles into liquid crystal structures has garnered considerable attention due to their unique electronic and structural properties. The [1,2,3]-triazole ring is a five-membered heterocycle that has become a focal point in the design of novel liquid crystal materials (Shanty et al., 2017). This interest is largely attributed to the triazole ring's ability to contribute to the overall rigidity of the molecular framework while simultaneously offering opportunities for extensive  $\pi$ -conjugation (Benbayer et al., 2013). Such properties are essential in enhancing the stability of mesophases and improving the overall performance of liquid crystal materials in various applications, including display technologies and

optoelectronic devices. Heterocyclic triazole ring can act as a significant compact mesogenic core that restricts the rotational freedom of BLCs and have attracted special attention due to the varying types of liquid crystalline phases and phenomena displayed, different from the traditional liquid crystals.

The synthesis of triazole-containing liquid crystals often involves click chemistry, particularly the copper(I)-catalyzed azide-alkyne cycloaddition (CuAAC), which is renowned for its efficiency, regioselectivity, and ability to produce 1,4-disubstituted triazole rings under mild conditions. This synthetic approach allows for the precise incorporation of triazole units into liquid crystal precursors, enabling the fine-tuning of their mesomorphic properties. Various studies have demonstrated that the inclusion of the triazole ring can significantly influence the thermal and optical properties of liquid crystals, often leading to enhanced mesophase stability and broader temperature ranges for liquid crystalline behaviour (Cheng et al., 2018).

Al-shargabi et al. (2020) have elucidated the correlation between the electrostatic interaction of the carbonyl linking group and the cholesteryl moiety in the absence of a triazole unit. This interaction influences the manifestation of the smectic A (SmA) phase. However, introducing the [1,2,3]-triazole within the core system results in the emergence of the smectic C (SmC) phase and several frustrated mesophases; thereby, it is said to have enhanced polar packing. They concluded that introducing a triazole core in the current system has effectively heightened the SmA\*-SmC\* transition compared to the non-triazole derivatives, where they exhibited N\*-SmA\* transitions. Both steric considerations and a central transverse dipole in the molecule influence the emergence of the SmC\* phase.

Furthermore, Hariprasad and Srinivasa (2015) also highlighted that when incorporating five- or six-membered heterocycles, they become integral components of the core in rod-shaped, bent-shaped, or disc-shaped liquid crystal molecules. The growing interest in mesomorphic heterocyclic compounds is attributed to their diverse structures and unique mesomorphic properties. The presence of the heteroatom in the triazole unit led to the increase in molecular dipole and dielectric anisotropy, thereby increasing the polarity, which enhances the electrostatic interactions between molecules. The enhanced electrostatic interaction allows efficient packing and thus increases mesomorphic stability.

Nguyen et al. (2017) studied how electric fields influence the orientation of bent-core liquid crystals featuring two [1,2,3]-triazolyl rings and a central benzene ring. By adding wedge-shaped groups to the aromatic core, they induced a columnar arrangement. These liquid crystals exhibited a hexagonal columnar phase at room temperature, which transformed into a disordered columnar phase with short-range order when heated. Dielectric and switching studies showed that the electric conduction behaviour was significantly affected by the orientation of the columnar domains.

Liquid crystal dimers incorporating the [1,2,3]-triazole moiety also display remarkable phase transition behaviour, with the position of the triazole ring within the rigid core and the nature of attached substituents playing the key roles in determining the type and stability of mesogenic phases (Yeap et al., 2013). The [1,2,3]-triazole ring serves not only as a desirable linkage group but also offers functional versatility, acting as hydrogen or halogen acceptors, precursors for ionic compounds, and ligands for metal coordination complexes (Ouyang et al., 2021).

## **2.4 Types of Liquid Crystals**

Liquid crystals have received continual attention from researchers, and they have been regarded also as soft condensed materials. There are two general classes of liquid crystals, namely, thermotropic liquid crystal, which shows the liquid crystalline state exclusively on different temperature and demonstrating its importance in electrooptical and temperature-based sensors application. Whereas lyotropic liquid crystals, of which the formation of liquid crystal phases is achieved and influenced by solvents are accentuated in biological aspects.

### **2.4.1 Lyotropic Liquid Crystals**

The lyotropic-type liquid crystal serves as a prominent illustration where amphiphilic molecules coexist in water, and a similar phenomenon can be observed by dispersing anisotropic colloidal particles in an isotropic liquid. These liquid crystals are comprised of amphiphilic molecules, with the polar heads oriented towards water, indicating hydrophilic properties (Sonin, 2018). In contrast, the long hydrocarbon tails of these molecules avoid contact with water, exhibiting hydrophobic characteristics as demonstrated in Figure 2.5. Amphiphilic molecules in solution can organize into various phases, such as lamellar structures (comprising of parallel layers) or micellar formations (consisting of circular- or cylindrical-shaped multimolecular clusters known as micelles). A notable example of lyotropic liquid crystals includes concentrated soap solutions.